J|A|C|S
ARTICLES
Published on Web 04/20/2006

New Palladium(II)−($\eta^{3/5}$- or η^1-Indenyl) and Dipalladium(I)−(μ,η^3-Indenyl) Complexes

Christine Sui-Seng,[†] Gary D. Enright,[‡] and Davit Zargarian*[,†]

Contribution from the Département de chimie, Université de Montréal, Québec, Canada H3C 3J7, and Steacie Institute for Molecular Sciences, National Research Council, Ottawa, Ontario, Canada K1A 0R6

Received February 7, 2006; E-mail: zargarian.davit@umontreal.ca

Abstract: Reaction of the dimeric species [(η^3-Ind)Pd(μ-Cl)]$_2$ (**1**) (Ind = indenyl) with NEt_3 gives the complex (η^{3-5}-Ind)Pd(NEt_3)Cl (**3**), whereas the analogous reactions with $BnNH_2$ (Bn = $PhCH_2$) or pyridine (py) afford the complexes *trans*-L_2Pd(η^1-Ind)Cl (L = $BnNH_2$ (**4**), py (**5**)). Similarly, the one-pot reaction of **1** with a mixture of $BnNH_2$ and the phosphine ligands PR_3 gives the mixed-ligand, amino and phosphine species (PR_3)($BnNH_2$)Pd(η^1-Ind)Cl (R = Cy (**6a**), Ph (**6b**)); the latter complexes can also be prepared by addition of $BnNH_2$ to (η^{3-5}-Ind)Pd(PR_3)Cl (R = Cy (**2a**), Ph (**2b**)). Complexes **6** undergo a gradual decomposition in solution to generate the dinuclear Pd^I compounds (μ,η^3-Ind)(μ-Cl)Pd_2(PR_3)$_2$ (R = Cy (**7a**), Ph (**7b**)) and the Pd^{II} compounds ($BnNH_2$)(PR_3)$PdCl_2$ (R = Cy (**8a**), Ph (**8b**)), along with 1,1′-biindene. The formation of **7** is proposed to proceed by a comproportionation reaction between in situ-generated Pd^{II} and Pd^0 intermediates. Interestingly, the reverse of this reaction, disproportionation, also occurs spontaneously to give **2**. All new compounds have been characterized by NMR spectroscopy and, in the case of **3**, **4**, **5**, **6a**, **7a**, **7b**, and **8a**, by X-ray crystallography.

Introduction

Studies on the structures and reactivities of Ind complexes (Ind = indenyl and its substituted or functionalized derivatives) have shown that the bonding mode adopted by the Ind ligand and its net electronic contribution to the metal center in a given complex depend strongly on the electronic configuration of the metal (d^n) and its formal electron count. Thus, the formally electron-deficient complexes of early metals (d^{0-5}, up to 18 valence electrons) generally favor greater hapticities (η^5-Ind),[1] whereas the more electron-rich late metal centers (d^{6-8}, 16−18 valence electrons) favor lower hapticities and display various degrees of "slip-fold" distortions (η^{1-5}-Ind). This flexible and responsive nature of M−Ind bonding, the so-called "indenyl effect", is believed to facilitate a number of interesting stoichiometric and catalytic reactions.[2]

Most of the studies carried out to date on Ind complexes have focused on compounds of groups 4−9 transition metals, such that the chemistry of group 10 metal−indenyl complexes is much less explored. Nevertheless, a number of studies carried out over the past decade on Ni^{II}−Ind complexes IndNi(L)X and [IndNi(L)L′]$^+$ have shown that the Ind ligand is more slip-folded in these complexes in comparison to the complexes Ind−M^I-(L)L′ of group 9 metals, despite the similar (formal) electron counts of the metal centers in these complexes (d^8, 18 electrons).[3] Some of these Ni−Ind complexes are also competent precatalysts for the oligo- and polymerization of alkenes,[4] alkynes,[5] and $PhSiH_3$,[6] and for the hydrosilylation of olefins.[4f,k,7]

The interesting structural characteristics and catalytic reactivities promoted by Ni−Ind compounds and the relatively

[†] Université de Montréal.
[‡] National Research Council Canada.

(1) For Ind complexes featuring unusually large hapticities, see: (a) Bradley, A. C.; Lobkovsky, E.; Chirik, P. J. *J. Am. Chem. Soc.* **2003**, *125*, 8110. (b) Bradley, A. C.; Keresztes, I.; Lobkovsky, E.; Young, V. G.; Chirik, P. J. *J. Am. Chem. Soc.* **2004**, *126*, 16937. (c) Bradley, A. C.; Lobkovsky, E.; Keresztes, I.; Chirik, P. J. *J. Am. Chem. Soc.* **2005**, *127*, 10291.

(2) For representative reactivities of indenyl complexes see the following reports and references therein: (a) Frankom, T. M.; Green, J. C.; Nagy, A.; Kakkar, A. K.; Marder, T. B. *Organometallics* **1993**, *12*, 3688. (b) Gamasa, N. P.; Gimeno, J.; Gonzalez-Bernado, C.; Martin-Vaca, B. M.; Monti, D.; Bassetti, M. *Organometallics* **1996**, *15*, 302. (c) Foo, T.; Bergman, R. G. *Organometallics* **1992**, *11*, 1801. (d) Trost, B. M.; Kulawiec, R. J. *J. Am. Chem. Soc.* **1993**, *115*, 2027. (e) O'Connor, J. M.; Casey, C. P. *Chem. Rev.* **1987**, *87*, 307. (f) Marder, T. B.; Roe, C. D.; Milstein, D. *Organometallics* **1988**, *7*, 1451. (g) Halterman, R. L. *Chem. Rev.* **1992**, *92*, 965. (h) Hauptman, E.; Sabo-Etienne, S.; White, P. S.; Brookhart, M.; Garner, J. M.; Fagan, P. J.; Calabrese, J. C. *J. Am. Chem. Soc.* **1994**, *116*, 8038.

(3) For a recent review on the chemistry of group 10 metal−indenyl complexes, see: Zargarian, D. *Coord. Chem. Rev.* **2002**, *233*−*234*, 157.

(4) (a) Vollmerhaus, R.; Bélanger-Gariépy, F.; Zargarian, D. *Organometallics* **1997**, *16*, 4762. (b) Dubois, M.-A.; Wang, R.; Zargarian, D.; Tian, J.; Vollmerhaus, R.; Li, Z.; Collins, S. *Organometallics* **2001**, *20*, 663. (c) Groux, L. F.; Zargarian, D. *Organometallics* **2001**, *20*, 3811. (d) Groux, L. F.; Zargarian, D.; Simon, L. C.; Soares, J. B. P. *J. Mol. Catal. A* **2003**, *193* (1−2), 51. (e) Groux, L. F.; Zargarian D. *Organometallics* **2003**, *22*, 3124. (f) Groux, L. F.; Zargarian, D. *Organometallics* **2003**, *22*, 4759. (g) Sun, H.; Li, W.; Han, X.; Shen, Q.; Zhang, Y. *J. Organomet. Chem.* **2003**, *688*, 132. (h) Li, W.-F.; Sun, H.-M.; Shen, Q.; Zhang, Y.; Yu, K.-B. *Polyhedron* **2004**, *23*, 1473. (i) Jimenez-Tenorio, M.; Puerta, M. C.; Salcedo, I.; Valerga, P.; Costa, S. I.; Silva, L. C.; Gomes, P. T. *Organometallics* **2004**, *23*, 3139. (j) Sun, H. M.; Shao, Q.; Hu, D. M.; Li, W. F.; Shen, Q.; Zhang, Y. *Organometallics* **2005**, *24*, 331. (k) Gareau, D.; Sui-Seng, C.; Groux, L. F.; Brisse, F.; Zargarian, D. *Organometallics* **2005**, *24*, 4003.

(5) (a) Wang, R.; Bélanger-Gariépy, F.; Zargarian, D. *Organometallics* **1999**, *18*, 5548. (b) Wang, R.; Groux, L. F.; Zargarian D. *Organometallics* **2002**, *21*, 5531. (c) Wang, R.; Groux, L. F.; Zargarian, D. *J. Organomet. Chem* **2002**, *660*, 98. (d) Rivera, E.; Wang, R.; Zhu, X. X.; Zargarian, D.; Giasson, R. *J. Mol. Catal. A* **2003**, *204*−*205*, 325.

(6) (a) Fontaine, F.-G.; Kadkhodazadeh, T.; Zargarian, D. *J. Chem. Soc., Chem. Commun.* **1998**, 1253. (b) Fontaine, F.-G.; Zargarian, D. *Organometallics* **2002**, *21*, 401.

(7) Fontaine, F.-G.; Nguyen, R.-V.; Zargarian, D. *Can. J. Chem.* **2003**, *81*, 1299.

10.1021/ja060747a CCC: $33.50

Scheme 1

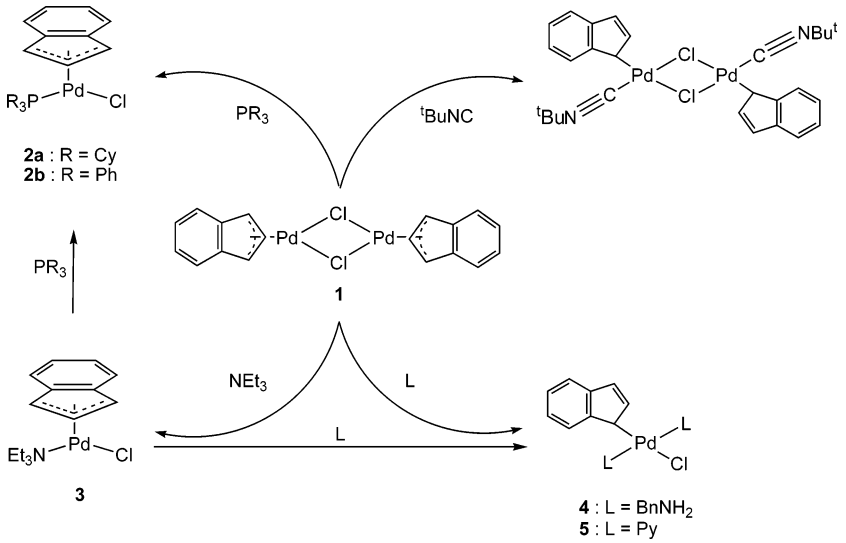

unexplored chemistry of their Pd analogues[8] have motivated us to initiate a systematic study of Pd−Ind compounds in order to elucidate the influence of the metal center on structures and reactivities. Our initial studies showed significantly lower Ind hapticities (more "slippage") in the compounds (η^{3-5}-Ind)Pd(PR$_3$)Cl (R= Ph, Cy, Me, and OMe); moreover, replacing the PR$_3$ in these compounds by *t*-BuNC gave [(η^1-Ind)(*t*-BuNC))Pd(μ-Cl)]$_2$.[9] Subsequently, we undertook to synthesize a new series of complexes bearing Lewis bases other than phosphines and isocyanides to allow a comparison of structural and reactivity features as a function of both metal and the Lewis base ligand.

The present contribution reports on the syntheses of the Ind−Pd^{II}(amine) complexes (η^{3-5}-Ind)Pd(NEt$_3$)Cl), (η^1-Ind)Pd(BnNH$_2$)$_2$Cl (Bn = PhCH$_2$), and (η^1-Ind)Pd(py)$_2$Cl (py = pyridine). The subsequent reaction of these complexes with phosphines has given access to new Pd^{I}−Pd^{I} complexes bearing a bridging indenyl ligand, i.e., (μ,η^3-Ind)(μ-Cl)Pd$_2$(PR$_3$)$_2$ (R = Ph, Cy). Several dinuclear Pd^{I}−Pd^{I} complexes featuring μ-allyl or μ-cyclopentadienyl ligands are known,[10] whereas [(μ,η^3-Ind)Pd(CNR)]$_2$ represent the only μ-Ind complexes reported previously.[8c,d]

Results and Discussion

Reaction of the Dimer [(η^3-Ind)Pd(μ-Cl)]$_2$ (1) with Amines. The synthetic route developed for the preparation of phosphine and isocyanide complexes (η-Ind)Pd(PR$_3$)Cl (**2**) and [(η^1-Ind)(*t*-BuNC))Pd(μ-Cl)]$_2$ (Scheme 1)[9a] was used to prepare the target amino complexes. Thus, stirring a suspension of **1**[11] in benzene with NEt$_3$ gave the complex (η-Ind)Pd(NEt$_3$)Cl (**3**), whereas the analogous reactions with BnNH$_2$ and py gave the η^1-Ind complexes (η^1-Ind)Pd(BnNH$_2$)$_2$Cl (**4**) and (η^1-Ind)Pd(py)$_2$Cl (**5**), respectively (Scheme 1). The new complexes were isolated in 70−75% yields as brown (**3**) or yellow-brown (**4** and **5**) solids; the latter compounds were also prepared in ca. 85% yield via the reaction of **3** with 1 or 2 equiv of BnNH$_2$ or py (Scheme 1). All three complexes are thermally stable and can be handled in air, both in the solid state and in solution, without appreciable decomposition. Their identities were deduced from their NMR spectra and confirmed by the results of elemental analyses and single-crystal X-ray diffraction studies, as described below.

Characterization of 3−5 by NMR. The ambient-temperature ^{1}H NMR spectrum of (η-Ind)Pd(NEt$_3$)Cl (**3**) displayed relatively broad signals for all Ind protons, but a better resolution was obtained at −10 °C. The assignment of the ^{1}H and ^{13}C {^{1}H} NMR spectra was facilitated by selective homodecoupling, inverse-gated decoupling, COSY, and HMQC experiments. The selective 1D NOESY experiment correlated the methylene groups of NEt$_3$ with H3 and H4 at 4.61 and 6.45 ppm, respectively (see Figure 2 for the numbering scheme). Moreover, the high resolution of the ^{1}H NMR spectrum of **3** allowed us to observe the detailed multiplicities of these signals and to determine the various H−H coupling constants, as follows: $^3J_{H1-H2} \approx {}^3J_{H2-H3} \approx {}^4J_{H1-H3} \approx$ 2.4 Hz; $^4J_{H1-H7} \approx {}^4J_{H3-H4} \approx$ 0.8 Hz; $^5J_{H3-H5} \approx {}^5J_{H1-H6} \approx$ 1.2 Hz.

Overall, the chemical shifts and the multiplicities of the signals for the Ind protons in **3** follow a pattern commonly observed for the previously studied (η-Ind)Pd(PR$_3$)Cl analogues.[9] For instance, the signals for H1 (5.59 ppm) and H3 (4.61 ppm) are both strongly shielded in comparison to the other Ind signals (6.31−6.93 ppm). On the other hand, the ^{13}C chemical shifts of C1 and C3 (ca. 73 vs 82 ppm) indicate a somewhat higher shielding for C1, which is the opposite of our

(8) To our knowledge, the following are the only Pd−Ind compounds reported prior to our studies: [(η^3-Ind)Pd(μ-Cl)]$_2$,[8a,b] [(μ,η^3-Ind)Pd(CNR)]$_2$ (R = *t*-Bu, 2,6-(CH$_3$)$_2$C$_6$H$_3$; 2,4,6-(CH$_3$)$_3$C$_6$H$_2$; 2,4,6-(t-Bu)$_3$C$_6$H$_2$),[8c,d] (η^3-Ind)Pd(PMe$_3$)(CH(SiMe$_3$)$_2$),[8e,f] and [(η^3-Ind)PdL$_2$]$^+$ (L$_2$ = bipy, tmeda).[8g,h] A preliminary communication has also appeared on the preparation of a series of Ind derivates from the reaction of cyclopropene and (PhCN)$_2$PdCl$_2$.[8i] (a) Nakasuji, K.; Yamaguchi, M.; Murata, I.; Tatsumi, K.; Natamura, A. *Organometallics* **1984**, *3*, 1257. (b) Samuel, E.; Bigorgne, M. *J. Organomet. Chem.* **1969**, *19*, 9. (c) Tanase, T.; Nomura, T.; Yamamoto, Y.; Kobayashi, K. *J. Organomet. Chem.* **1991**, *410*, C25. (d) Tanase, T.; Nomura, T.; Fukushina, T.; Yamamoto, Y.; Kobayashi, K. *Inorg. Chem.* **1993**, *32*, 4578. (e) Alias, F. M.; Belderrain, T. R.; Paneque, M.; Poveda, M. L.; Carmona, E. *Organometallics* **1998**, *17*, 5620. (f) Alias, F. M.; Belderrain, T. R.; Carmona, E.; Graiff, C.; Paneque, M.; Poveda, M. L. *J. Organomet. Chem.* **1999**, *577*, 316. (g) Vicente, J.; Abad, J.-A.; Bergs, R.; Jones, P. G.; De Arellano, M. C. R. *Organometallics* **1996**, *15*, 1422. (h) Vicente, J.; Abad, J.-A.; Bergs, R.; De Arellano, M. C. R.; Martinez-Vivente, E.; Jones, P. G. *Organometallics* **2000**, *19*, 5597. (i) Fiato, R. A.; Mushak, P.; Battiste, M. A. *Chem. Commun.* **1975**, 869.

(9) (a) Sui-Seng, C.; Enright, G. D.; Zargarian, D. *Organometallics* **2004**, *23*, 1236. (b) Sui-Seng, C.; Groux, L. F.; Zargarian, D. *Organometallics* **2006**, *25*, 571.

(10) For reviews on Pd(I)−Pd(I) compounds, see: (a) Murahashi, T.; Kurosawa, H. *Coord. Chem. Rev.* **2002**, *231*, 207. (b) Werner, *Adv. Organomet. Chem.* **1981**, *19*, 155.

(11) For the original synthesis of this dimeric compound see refs 8a,b above. For a revised synthesis see ref 9a.

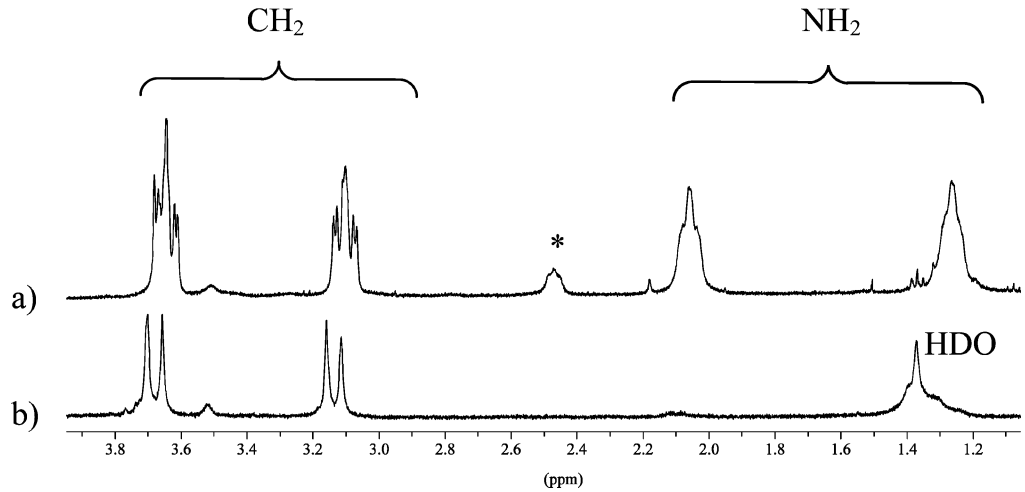

Figure 1. (a) 400 MHz ^{1}H NMR spectrum of complex **4** in C_6D_6, showing the four multiplets of the C*H*$_2$N*H*$_2$ protons (*, impurities). (b) ^{1}H NMR spectrum of complex **4** in C_6D_6/D_2O.

previous observations for Ni− and Pd−Ind complexes bearing phosphines. For example, the chemical shifts of these nuclei in (η-Ind)Pd(PR_3)Cl are in the range of 94−113 ppm for C1 and 70−80 ppm for C3, indicating that the hybridization is more sp^2-like at C1 and more sp^3-like at C3; we have argued that these observations are consistent with the larger trans influence of PR_3 versus Cl.[9a] Accordingly, we attribute the observation of a more shielded C1 in **3** to a more sp^3-like hybridization at C1 arising from the weaker trans influence of NEt_3 versus Cl. The latter phenomenon is reflected in the solid-state structure of this complex, which shows that Pd−C1 < Pd−C3 (vide infra), but the fairly downfield chemical shift of H1 (ca. 5.6 ppm) is not consistent with sp^3 C1.

The ^{1}H and ^{13}C{^{1}H} NMR spectra of complexes **4** and **5** showed only one set of signals, indicating that only one isomer, cis or trans, was obtained in each case; we have assumed that these complexes adopt the thermodynamically more stable trans geometry, as in bis(amine)dihalogenopalladium(II) complexes.[12] The NMR data for the indenyl fragment were very similar to those found in previously reported transition metal−η^1-indenyl complexes.[8e,9a,13] In the ^{13}C NMR spectra, for instance, the chemical shift of C1 is significantly upfield of the corresponding signals in η-Ind complexes **2** (40 vs 94−113 ppm). The signals for the diastereotopic PhC*H*$_2$N*H*$_2$ protons in complex **4** appear as four triplets of doublets centered at 3.84, 3.34, 2.37, and 1.61 ppm (Figure 1a). The H,H-COSY spectrum indicates that these signals form an ABCD spin system. The vicinal and geminal coupling constants were estimated at ca. 3 and 12 Hz, respectively. Unambiguous assignment of the amine protons was achieved by adding a few drops of D_2O to the NMR sample, which caused the two multiplets observed for N*H*$_2$ at 2.37 and 1.61 ppm to disappear (Figure 1b). The NH/ND exchange also reduced the two C*H*$_2$ signals to an AB doublet, and this allowed us to determine the geminal coupling constant for these protons ($^2J_{AB} \approx 12$ Hz).

Solid-State Structures of 3−5. The X-ray analyses of **3**−**5** have confirmed the spectral assignments and provided valuable structural information for these first Ind−Pd complexes bearing amine ligands. The crystal data and selected structural parameters are presented in Tables 1 and 2, and the ORTEP diagrams are shown in Figures 2 and 3, respectively. The overall geometry is approximately square planar in complex **3**, with the largest distortion arising from the small C1−Pd−C3 angle of 62°. The Pd−N distance of 2.225(2) Å is in the range of Pd−N bond lengths reported to date for Pd−NEt_3 complexes.[14] The fairly long Pd−C3a and Pd−C7a distances indicate that the Ind−Pd interaction is primarily through the allylic carbons C1, C2, and C3. The significant difference in the Pd−C bond lengths is a reflection of the so-called "slippage" of the Ind ligand, which can be measured by calculating parameters such as the slip value (ΔM−C) and the hinge and fold angles (HA and FA).[15] The calculated values of these parameters in **3**, 0.39 Å and ca. 16 and 12°, respectively, are similar to the corresponding values in the phosphine analogues (η^{3-5}-Ind)Pd(PR_3)Cl (**2**) but significantly smaller than those of [(η^3-Ind)Pd(μ-Cl)]$_2$ (**1**) (ΔM−C = 0.46 Å, HA = 17°, FA = 16°).[9a] On the other hand, the significant asymmetry in the Pd−C(allyl) bond lengths (Pd−C1 < Pd−C3) is the opposite of the trend generally observed in phosphine complexes (Pd−C1 > Pd−C3), thus confirming the trans influence order deduced from the NMR spectra (PR_3 > Cl > NEt_3).

X-ray crystal structure analyses of complexes **4** and **5** have confirmed the trans square planar geometry around Pd (Figure 3). The structural parameters for these complexes are similar to those found in the only other structurally characterized (η^1-Ind)Pd complex,[8a] as well as those of other η^1-Ind compounds reported previously.[16,17] For example, the sp^3-hybridized character of the Pd-bound carbon atom is reflected in the C1−C7a (ca. 1.50 Å) and C1−C2 (ca. 1.47 Å) distances that are in the normal range for C−C single bonds, whereas the C2−C3

(12) Coe, J. C.; Lyons, R. J. *Inorg. Chem.* **1970**, *9*, 1775.

(13) (a) Casey, C. P.; O'Connor J. M *Organometallics* **1985**, *4*, 384. (b) Hermmann, W. A.; Kuhn, F. E.; Romao, C. C. *J. Organomet. Chem.* **1995**, *489*, C56. (c) O'Hare, D. *Organometallics* **1987**, *6*, 1766.

(14) To our knowledge, only two examples of Pd−NEt_3 complexes were characterized by single-crystal X-ray crystallography: $(Et_3N)_2PdCl_2$ (Timokhin, V. I.; Anastasi, N. R.; Stahl, S. S. *J. Am. Chem. Soc.* **2003**, *125*, 12996) and [Pd(dmpe)(Me)(NEt_3)][BPh_4] (Seligson, A. L.; Trogler, W. C. *J. Am. Chem. Soc.* **1991**, *113*, 2520).

(15) ΔM−C = 0.5 {(M−C3a + M−C7a) − 0.5 {(M−C1 + M−C3). HA is the angle between the planes encompassing the atoms C1, C2, C3 and C1, C3, C3a, C7a. FA is the angle between the planes encompassing the atoms C1, C2, C3 and C3a, C4, C5, C6, C7, C7a. The ΔM−C, HA, and FA values for a range of Ind complexes are given in the following reports: (a) Baker, T.; Tulip, T. H. *Organometallics* **1986**, *5*, 839. (b)Westcott, S. A.; Kakkar, A. K.; Stringer, G.; Taylor, N. J.; Marder, T. B. *J. Organomet. Chem.* **1990**, *394*, 777. The corresponding data for group 10 complexes are given in ref 3.

Table 1. Crystal Data, Data Collection, and Structure Refinement Parameters of **3**−**5** and **6a**

	3	**4**	**5**	**6a**
formula	$C_{15}H_{22}N_1Cl_1Pd_1$	$C_{23}H_{25}N_2Cl_1Pd_1.0.5C_6H_6$	$C_{19}H_{17}N_2Cl_1Pd_1$	$C_{34}H_{49}N_1P_1Cl_1Pd_1$
mol wt	358.19	510.35	415.20	644.56
cryst color, habit	brown-orange, block	yellow, plate	orange, block	orange, block
cryst dimens, mm	0.08 × 0.23 × 0.53	0.06 × 0.15 × 0.15	0.19 × 0.28 × 0.38	0.11 × 0.15 × 0.30
system	monoclinic	triclinic	orthorombic	triclinic
space group	$P2_1/c$	$P\bar{1}$	*Pbca*	$P\bar{1}$
a, Å	8.7756(1)	8.1918(13)	13.2654(2)	10.3658(1)
b, Å	13.9797(2)	10.3940(16)	13.3187(2)	12.3444(1)
c, Å	12.4209(1)	14.768(16)	19.3102(4)	14.4307(2)
α, deg	90	83.970(3)	90	91.696(1)
β, deg	95.397(1)	76.233(3)	90	109.563(1)
γ, deg	90	69.495(3)	90	100.612(1)
volume, Å^3	1517.04(3)	1143.6(3)	3411.69(10)	1701.87(3)
Z	4	2	8	2
D(calcd), g cm^{-1}	1.568	1.482	1.617	1.258
diffractometer	Bruker AXS, SMART 2K	Bruker AXS, SMART 1K	Bruker AXS, SMART 2K	Bruker AXS, SMART 2K
temp, K	100	125	100	100
λ, Å	1.54178	0.71073	1.54178	1.54178
μ, mm^{-1}	11.331	0.943	10.201	5.709
scan type	*ω* scan	*ω* scan	*ω* scan	*ω* scan
F(000)	728	522	1664	676
θ_{max}, deg	72.91	29.22	72.92	72.85
h,*k*,*l* range	$-10 \le h \le 10$	$-11 \le h \le 11$	$-16 \le h \le 15$	$-12 \le h \le 12$
	$-17 \le k \le 17$	$-14 \le k \le 14$	$-15 \le k \le 16$	$-14 \le k \le 15$
	$-15 \le l \le 14$	$-20 \le l \le 20$	$-23 \le l \le 23$	$-17 \le l \le 17$
no. of reflns collected/unique	18428/3002	14017/6119	26119/3389	20599/6482
absorption	multiscan	multiscan	multiscan	multiscan
correction	SADABS	SADABS	SADABS	SADABS
T (min, max)	0.16, 0.56	0.86, 0.94	0.09, 0.31	0.43, 0.64
$R\,[F^2 > 2\sigma(F^2)]$, $R_w(F^2)$	0.0280, 0.0735	0.0370, 0.0951	0.0470, 0.1275	0.0478, 0.1459
GOF	1.043	1.053	0.967	1.139

Table 2. Selected Bond Distances (Å) and Angles (deg) for **3**−**5** and **6a**

	3 (X = N, Y = C3)	**4** (X = N1, Y = N3)		**5** (X = N1, Y = N2)		**6a** (X = N, Y = P)
Pd−X	2.1674(18)	2.066(3)	2.061(3)	2.031(4)		2.129(3)
Pd−Cl	2.3598(5)	2.3996(8)		2.479(4)	2.278(4)	2.3812(9)
Pd−Y	2.225(2)	2.066(2)		2.036(4)		2.2752(9)
Pd−C1	2.151(2)	2.086(3)		2.054(10)	2.145(12)	2.110(4)
Pd−C2	2.171(2)					
Pd−C3a	2.608(2)					
Pd−C7a	2.548(2)					
C1−C2	1.403(4)	1.473(4)		1.465(12)	1.481(14)	1.490(5)
C2−C3	1.406(3)	1.352(5)		1.35(2)	1.35(3)	1.359(6)
C3−C3a	1.474(3)	1.457(4)		1.45(2)	1.37(5)	1.456(6)
C3a−C7a	1.422(3)	1.414(4)		1.423(10)	1.43(3)	1.426(5)
C7a−C1	1.480(3)	1.482(4)		1.493(14)	1.494(14)	1.472(5)
C3a−C4	1.383(4)	1.394(4)		1.341(13)	1.360(14)	1.391(5)
C4−C5	1.396(3)	1.386(5)		1.465(12)	1.461(15)	1.387(6)
C5−C6	1.386(4)	1.396(5)		1.372(13)	1.362(16)	1.408(7)
C6−C7	1.399(4)	1.390(5)		1.40(2)	1.41(2)	1.395(6)
C7−C7a	1.385(3)	1.390(4)		1.39(2)	1.41(2)	1.395(5)
X−Pd−Cl	93.19(5)	92.39(11)	81.32(18)	91.23(14)	86.67(14)	82.84(9)
C1−Pd−X	166.93(8)	87.11(14)	98.2(2)	91.9(3)	91.0(3)	89.84(14)
C1−Pd−Y	62.32(9)	91.6(1)		89.2(3)	88.9(3)	95.15(11)
Cl−Pd−Y	159.79(7)	88.91(7)		87.90(15)	93.27(16)	92.22(3)
C3−Pd−N	106.42(8)					
C1−Pd−Cl	97.61(7)					
ΔM−C (Å)[a]	0.39					
HA (deg)[b]	16.46					
FA (deg)[c]	12.71					

[a] ΔM−C = 0.5(M−C3a + M−C7a) − 0.5(M−C1 + M−C3). [b] Angle formed between the planes formed by the atoms C1, C2, C3 and C1, C3, C3a, C7a. [c] Angle formed between the planes formed by the atoms C1, C2, C3 and C3a C4, C5, C6, C7, C7a.

distance (ca. 1.35 Å) is in the expected range for a C(sp^2)−C(sp^2) double bond. The Pd−N bond lengths (ca. 2.06 Å for **4** and 2.03 Å for **5**) lie well within the range of distances reported previously for analogous compounds.[18] The coordinated pyridine rings in complex **5** form a dihedral angle of ca. 15° and are oriented nearly orthogonal to the Pd square plane, which serves, presumably, to maximize Pd→py back-bonding and minimize steric interactions.

New Monometallic (η^1-Ind)Pd^{II} and Bimetallic (μ,η^3-Ind)-Pd$^{I}_2$ Complexes. That complexes featuring η^{3-5}- or η^1-Ind

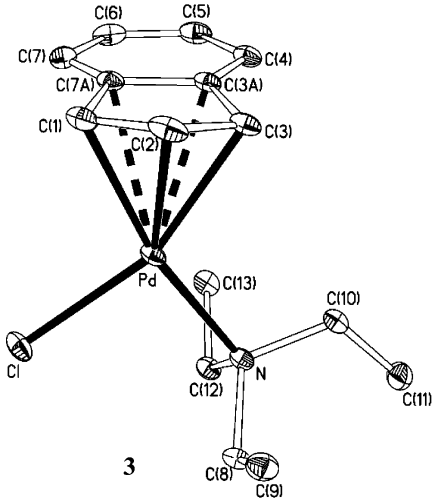

Figure 2. ORTEP views of complex **3**. Thermal ellipsoids are shown at 30% probability, and hydrogen atoms are omitted for clarity.

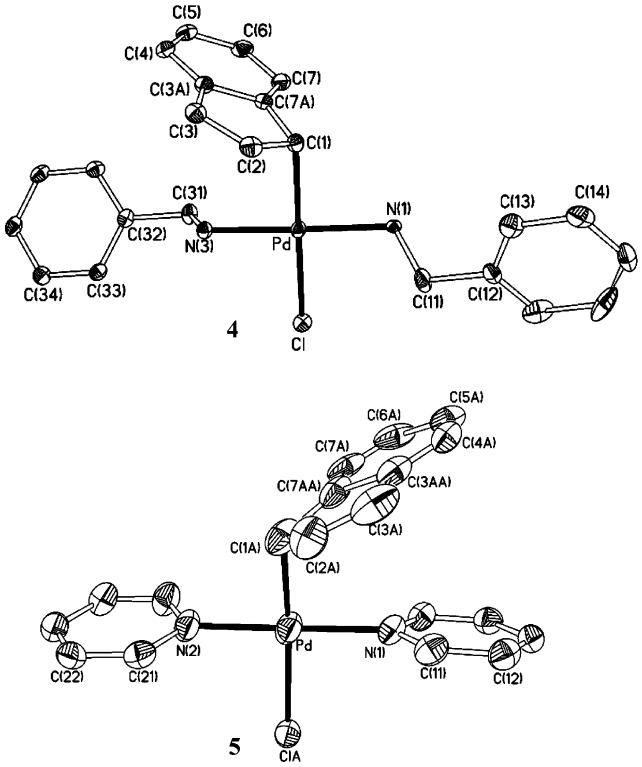

Figure 3. ORTEP views of complexes **4** and **5**. Thermal ellipsoids are shown at 30% probability, and hydrogen atoms and the solvent molecule are omitted for clarity. The $BnNH_2$ in **4** and the Ind and Cl ligands in **5** are each disordered over two positions; the views shown in this figure represent the major model.

ligands can be prepared from the reaction of the common precursor **1** with various ligands L (PR_3, NEt_3, *t*-BuNC, $BnNH_2$, py; Scheme 1) shows unambiguously that the nature of the incoming ligand L has a direct bearing on Ind hapticity in the product. To determine how the Ind hapticity would change with a mixture of ligands, we added 2 equiv of PR_3 to a CH_2Cl_2 solution of **4**, generated in situ by addition of 2 equiv of $BnNH_2$ to **1**. The reaction with PCy_3 gave an orange-brown solution from which we isolated an orange powder that was identified as the mixed-ligand species (η^1-Ind)Pd(PCy_3)($BnNH_2$)Cl (**6a**, Scheme 2, method A, 85% yield). The analogous reaction with PPh_3 gave (η^1-Ind)Pd(PPh_3)($BnNH_2$)Cl (**6b**), which was characterized by NMR but could not be isolated and purified because it decomposed to two new products that will be discussed later (Scheme 2). Complexes **6a** and **6b** were also obtained by adding 1 equiv of $BnNH_2$ to (η-Ind)Pd(PCy_3)Cl (**2a**) or its PPh_3 analogue **2b**, respectively (Scheme 2, method B, ca. 78% yield for **6a**).

The new η^1-Ind complexes **6** can be considered to be suitable models for the postulated intermediate in the ligand displacement reaction (η-Ind)M(L)Cl + L′ → (η-Ind)M(L′)Cl + L, proceeding by an associative mechanism. It is interesting to note that associative ligand substitutions of the closely related complexes (η-Ind)M(L)$_2$ of group 9 metals are believed to proceed via η^3-Ind intermediates (e.g., (η^3-Ind)Ir(PMe_2Ph)$_3$).[19] One possible explanation for the apparently different behaviors of these d^8 metal centers is that, in each case, the intermediate species maintains the electronic configuration of its precursor complex; thus, the (η^1-Ind)Pd^{II} and (η^3-Ind)Ir^{I} species both maintain the (nearly) 16- and 18-electron configurations of their respective predecessors.

As mentioned above, after a few hours, complex **6b** decomposes fairly rapidly to give two new products. Complex **6a** was found to have greater thermal stability, but it too decomposed gradually (over 24 h) to give a solid residue which gave a mixture of crystals upon recrystallization. Visual inspection of this mixture under a microscope showed two different crystals, orange microcrystals and larger yellow-orange crystals, which were separated mechanically and identified by X-ray diffraction analyses as (μ,η^3-Ind)(μ-Cl)$Pd_2(PCy_3)_2$ (**7a**) and ($BnNH_2$)-(PCy_3)$PdCl_2$ (**8a**), respectively. The products arising from the decomposition of **6b** were found to be PPh_3 analogues of **7a** and **8a**. In this case, recrystallization of the solid residues from CH_2Cl_2/hexane did furnish pure samples of (μ,η^3-Ind)(μ-Cl)-$Pd_2(PPh_3)_2$ (**7b**) in ca. 50% yield, but samples of the second product, **8b**, were always contaminated with **7b** and could not be obtained in pure form. We have probed the various reaction pathways that convert **1**, **2**, or **6** into complexes **7** and **8**, and have examined briefly the stabilities and reactivities of the latter; these studies are discussed next. The characterization of the new complexes **6**−**8** will be discussed in the following section.

The analogous reactions of **5** with phosphines or the reaction of **2** with py gave complex mixtures, which were analyzed by NMR and shown to contain the following species: **2a**, (η^1-Ind)Pd(PCy_3)(py)Cl, $(PCy_3)_2PdCl_2$, **7a**, and biindene in the PCy_3 reactions; $(PPh_3)_2PdCl_2$, **7b**, and biindene in the PPh_3 reactions. Isolation of the products from these mixture was not pursued.

(16) (a) Guérin, F.; Beddie, C. L.; Stephan, D. W.; v. H. Spence, E.; Wurz, R. *Organometallics* **2001**, *20*, 3466. (b) Deck, P. A.; Fronczek, F. R. *Organometallics* **2000**, *19*, 327. (c) Blenkiron, P.; Enright, G. D.; Taylor, N. J.; Carty, A. J. *Organometallics* **1996**, *15*, 2855. (d) Thorn, M. G.; Fanwick, P. E.; Chesnut, R. W.; Rothwell, I. P. *Chem. Commun.* **1999**, 2543. (e) Radius, U.; Sundermeyer, J.; Peters, K.; v. Schering, H. G. Z. *Anorg. Allg. Chem.* **2002**, *628*, 1226.

(17) For a detailed discussion of η^1-Ind complexes, see: Stradiotto, M.; McGlinchey, M. J. *Coord. Chem. Rev.* **2001**, *219*−221, 311.

(18) For examples on X-ray structures of *trans*-bis(benzylamine)palladium(II) complexes, see: (a) Sui-Seng, C.; Zargarian, D. *Acta Crystallogr.* **2003**, *E59*, m957. (b) Decken, A.; Pisegna, G. L.; Vogels, C. M.; Westcott, S. A. *Acta Crystallogr.* **2000**, *C56*, 1071. For examples on X-ray structures of *trans*-bis(pyridine)palladium(II) complexes, see: (c) Viossat, B.; Dung, N.-H.; Robert, F. *Acta Crystallogr.* **1993**, *C49*, 84. (d) Cheshkov, D. A.; Belyaev, B. A.; Belov, A. P.; Rybakov, V. B. *Acta Crystallogr.* **2004**, *E60*, m300.

(19) Merola, J. S.; Kacmarcik, R. T.; Van Engen, D. *J. Am. Chem. Soc.* **1986**, *108*, 329.

Scheme 2

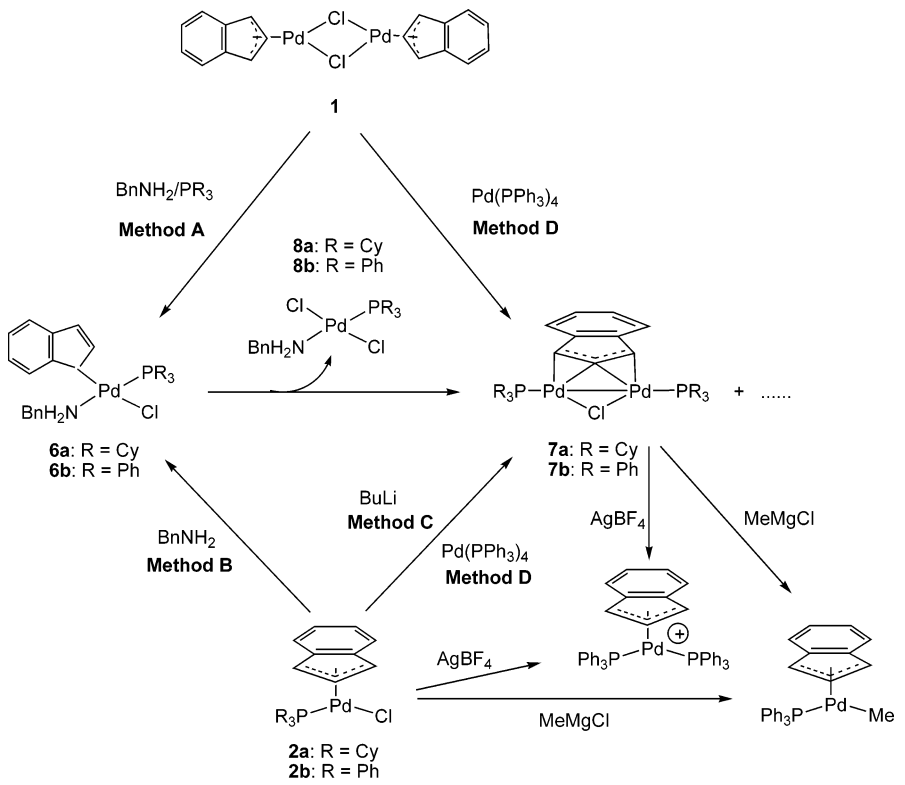

The bimetallic $(\mu,\eta^3\text{-Ind})Pd^{I}_2$ compounds **7** are reminiscent of the analogous Cp complex $(\mu,\eta^3\text{-Cp})(\mu\text{-Cl})Pd_2(P^iPr_3)_2$, which are prepared by reacting $CpPd(P^iPr_3)Cl$ with the reducing agent Mg, the hydrides $LiAlH_4$ or $NaBH_4$, or the alkylating agent *n*-BuMgBr.[20] By analogy to the latter route, we reacted **2a** and **2b** with 0.5 equiv of BuLi in NMR-scale reactions to test whether bimetallic **7** could be obtained in this way. The ^1H NMR spectra of these reactions contained the expected signals for **7**, in addition to signals attributed to 1-butene and free indene (Scheme 2, method C). Monitoring the reaction by $^{31}P\{^1H\}$ NMR spectroscopy showed the appearance, during the initial stages of the reaction, of new signals at ca. δ 49 (PCy_3 species) and 41 ppm (PPh_3 species), followed by a gradual disappearance of these signals and the emergence of the corresponding signals for **7**. We propose that these species are $Pd^{II}-Bu$ intermediates whose decomposition by β-H elimination gives 1-butene and $Pd^{II}-H$ species. The latter are not detected due to a rapid reductive elimination that generates free indene and $Pd^0(PR_3)_n$ species. The formation of **7** likely proceeds by a comproportionation reaction between the in situ-generated Pd^0 species and the Pd^{II} precursors **2** (Scheme 3). It is noteworthy that direct comproportionation reactions between organopalladium(II) and Pd^0 species have been used to prepare many different Pd^{I} species, including dipalladium(I) compounds featuring $(\mu,\eta^3\text{-Cp})$ and $(\mu,\eta^3\text{-allyl})$ ligands.[10] Accordingly, we found that a direct reaction between $Pd(PPh_3)_4$ and **1** or **2b** gives **7b** (Scheme 2, method D), thus confirming that a comproportionation reaction can lead to analogous $(\mu,\eta^3\text{-Ind})$ compounds.

The above observations allow us to rationalize the unanticipated formation of **7** and **8** from **6** via the sequence of steps shown in Scheme 4. First, **6** undergoes a ligand redistribution process to give the bis(chloro) compounds $(BnNH_2)(PR_3)PdCl_2$ (**8**) and the bis(η^1-Ind) complexes $(\eta^1\text{-Ind})_2Pd(PR_3)(BnNH_2)$ (step a). The latter decompose via reductive elimination to give 1,1′-biindene (Ind−Ind) and $Pd^0(PR_3)_n(BnNH_2)_m$ (step b). A comproportionation reaction between the latter and **6** generates the $(\mu,\eta^3\text{-Ind})Pd^{I}_2$ species **7** (step c). The side product Ind−Ind has been detected in the reaction mixtures by ^1H NMR of the solutions of **6** (over 24 h), and GC/MS analyses have confirmed its presence ($M^{\bullet+}$ at *m*/*z* 230). Moreover, some of this side product gets dehydrogenated to *trans*-1,1′-bis(indenylidene) (Ind═Ind),[21] which cocrystallized with **7a** (vide infra). We speculate that this dehydrogenation proceeds by addition of the benzylic C−H bond of Ind−Ind to the in situ-generated Pd^0 species to give $(\eta^1\text{-(1-Ind-Ind)})Pd(H)(PR_3)(BnNH_2)$ (step d). β-H elimination of the latter generates Ind═Ind and a bis(hydrido) species (step e) that regenerates the original Pd^0 species by eliminating H_2 (step f, Scheme 4).

Scheme 3

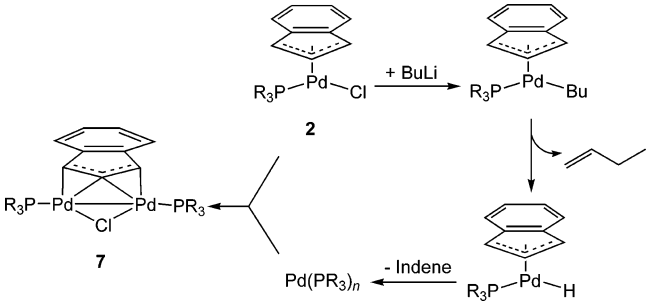

Solid samples of the μ,η^3-Ind compounds **7** can be handled in air indefinitely, but in solution they undergo a gradual and irreversible transformation (over several weeks) into the cor-

(20) Felkin, H.; Turner, G. K. *J. Organomet. Chem.* **1977**, *129*, 429.

(21) Strictly speaking, the designation of *trans*-1,1′-bis(indenylidene) as Ind═Ind is not consistent with the definition of Ind as the indenyl radical C_9H_7, but this designation has been adopted for its simplicity and intuitive appeal.

Scheme 4

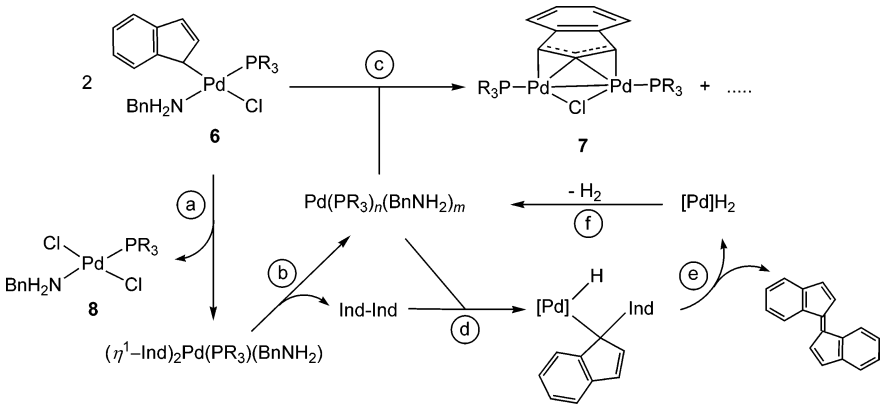

responding monomeric Pd^{II}−phosphine species (η-Ind)$Pd(PR_3)$-Cl (**2**). This observation seemed to indicate that complexes **7** behave as if they are simple combinations of the Pd^{II} compounds **2** and the $Pd^0(PR_3)$ fragment, rather than "real" dipalladium(I) species. Indeed, our preliminary results indicate that complexes **7** demonstrate reactivities virtually identical to those of **2**. For instance, reacting **7b** with $AgBF_4$ results in the formation of some black Pd residues and the monomeric complex [(η-Ind)-$Pd(PPh_3)_2$][BF_4] in 46% isolated yield; the latter compound is also obtained from the reaction of (η-Ind)$Pd(PPh_3)Cl$ (**2b**) with $AgBF_4$ (Scheme 2).[9b] Similarly, reacting MeMgCl with either **7b** or **2b** gives the same product, namely (η-Ind)$Pd(PPh_3)Me$.[9b] It appears, therefore, that the comproportionation reaction that generates complexes **7** can proceed in the reverse sense (disproportionation) to give complexes **2** and $Pd^0(PR_3)_n$.

Characterization of Complexes 6−8. Complexes **6a**, **7a**, **7b**, and **8a** were characterized by NMR spectroscopy, elemental analyses (except for **8a**), and single-crystal X-ray diffraction studies, whereas complexes **6b** and **8b** were identified by comparing their NMR spectra to those of their fully characterized PCy_3 analogues.

The ambient-temperature NMR spectra of **6a** and **6b** gave indications of a slow exchange process. For example, the $^{31}P\{^1H\}$ NMR spectra showed a broad singlet at 41.5 and 37.1 ppm, respectively; similarly, some of the ^1H and ^{13}C NMR signals were broadened and some were missing. Cooling the NMR sample to −10 °C resulted in the sharpening of the ^{31}P signals and the emergence in the ^1H and ^{13}C NMR spectra of new signals due to the PCy_3, $BnNH_2$, and η^1-Ind ligands (e.g., $\delta_{H1} = 4.94$ ppm for **6a** (d, $^3J_{H-P} = 5.4$ Hz) and 4.47 ppm for **6b** (d, $^3J_{H-P} = 7.6$ Hz); $\delta_{C1} = 38.9$ ppm for **6a** and 46.6 ppm for **6b**).

X-ray diffraction studies helped establish the identity of **6a** unambiguously. The ORTEP diagram for **6a** is shown in Figure 4, while Tables 1 and 2 list the crystallographic data and selected bond distances and angles. The essentially square planar geometry adopted by the Pd center in **6a** shows a slight tetrahedral distortion (e.g., C1−Pd−Cl ≈ 172°), which serves, presumably, to minimize steric interactions between the Ind and PCy_3 ligands. The Pd−N distance is much longer than the corresponding distance in **4**, presumably because of the much greater trans influence of PCy_3 versus $BnNH_2$. All the other distances and angles are comparable to those found in the η^1-Ind complexes **4** and **5**. Similarly, in the X-ray molecular structure of complex **8a** (Table 1, Figure 5), the Pd center adopts a distorted square planar geometry (e.g., Cl1−Pd−Cl2 ≈ 176°) and the Pd−N and Pd−P distances are very close to those observed for complex **6a**.

The decomposition of **6** to new compounds was indicated by the appearance in the $^{31}P\{^1H\}$ NMR spectrum of new signals at δ 38.5 (**7a**), 25.7 (**7b**), 44.1 (**8a**), and 28.6 (**8b**). The spectral patterns observed in the ^1H and $^{13}C\{^1H\}$ NMR spectra of the

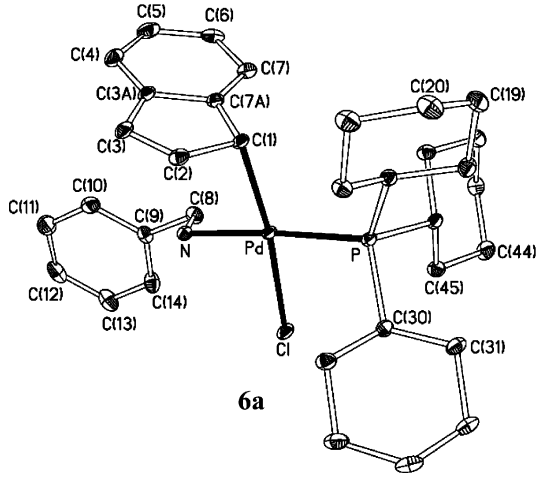

Figure 4. ORTEP view of complex **6a**. Thermal ellipsoids are shown at 30% probability, and hydrogen atoms are omitted for clarity.

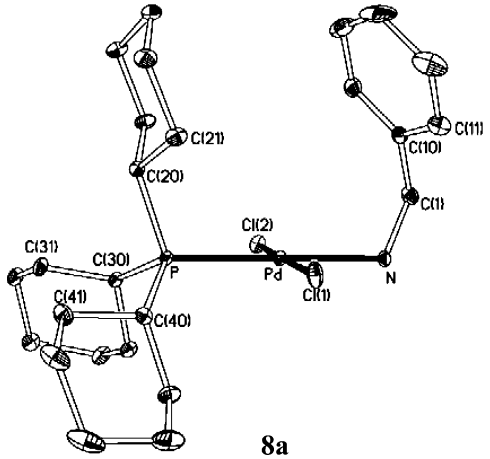

Figure 5. ORTEP view of complex **8a**. Thermal ellipsoids are shown at 30% probability, and hydrogen atoms are omitted for clarity. Selected bond lengths (Å) and angles (deg): Pd−Cl1 = 2.2951(5), Pd−Cl2 = 2.3068(5), Pd−N = 2.126(2), Pd−P = 2.2665(5), N−C1 = 1.489(3), P−Pd−Cl1 = 91.08(2), Cl1−Pd−N = 86.97(5), N−Pd−Cl2 = 88.85(5), Cl2−Pd−P = 93.09(2).

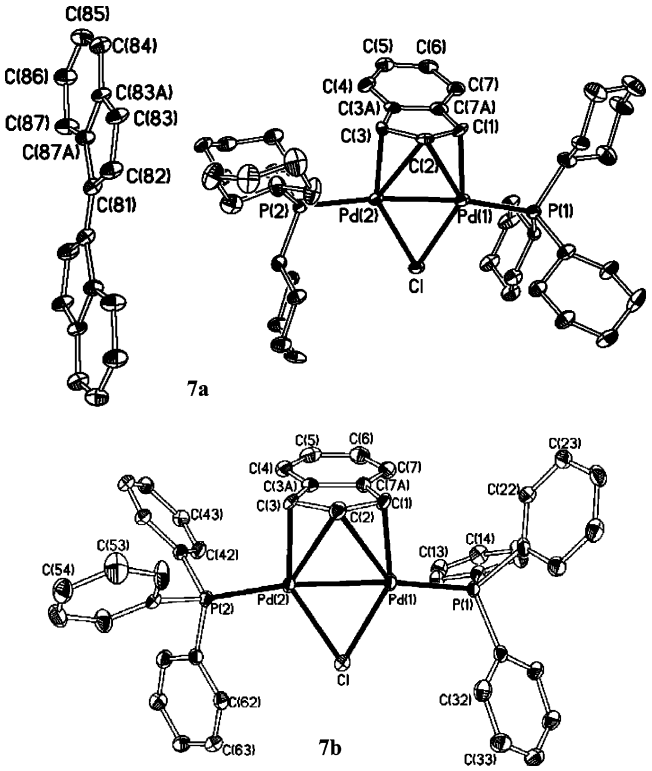

Figure 6. ORTEP views of complexes **7a** and **7b**. Thermal ellipsoids are shown at 30% probability, and hydrogen atoms are omitted for clarity.

μ,η^3-Ind moiety in **7a** and **7b** were very different from those of (η-Ind)Pd(PR_3)Cl complexes, but quite similar to the corresponding signals of the previously studied complexes [(μ,η^3-Ind)Pd(CNR)]$_2$.[8c,d] For instance, a set of signals corresponding to an AX_2 system was observed for H2 (4.22 ppm, quintuplet, $^3J_{H-H} = {}^3J_{H-P} = 3.6$ Hz) and H1/H3 (triplets of doublets at δ 5.81 ppm (**7a**) and 5.12 ppm (**7b**), $^3J_{H-P} = 7.3$ Hz, $^3J_{H-H} = 3.6$ Hz),[22] while H4−H7 displayed an A_2B_2 system ($\delta_{H4,7} =$ 7.04 ppm and $\delta_{H5,6} = 7.35$ ppm for **7a**; $\delta_{H4-7} = 6.52$ ppm and $\delta_{H5-6} = 5.98$ ppm for **7b**). This segment of the ^{1}H NMR spectrum for **7b** is shown in Figure 7. It should be noted that the chemical shifts for H4 and H7 in complex **7b** are much more upfield than those of H5 and H6, while the opposite trend is observed in **7a**. Inspection of the solid structure of **7b** has shown that H4 and H7 are fairly close to the center of one of the PPh_3 phenyl rings (vide infra), which indicates that the upfield shifts are likely caused by the anisotropy cone of the Ph rings. The $^{13}C\{^1H\}$ NMR spectra showed only five resonances, assigned to the four symmetry-related pairs of carbons C1/C3, C5/C6, C4/C7, C3a/C7a and C2; the assignments were facilitated by the HMQC spectra.

The X-ray molecular structures obtained for **7a** and **7b** are consistent with the NMR spectra observed in solution. The ORTEP diagrams for these compounds are shown in Figure 6, and the crystallographic data and selected bond distances and angles are listed in Tables 3 and 4. The coordination geometry around the Pd atoms in both complexes is square planar, displaying angular distortions of 5−30°. The structures consist of two Pd^I centers coordinated by a terminal phosphine ligand (Pd−P ≈ 2.26−2.29 Å) and bridged by a μ,η^3-Ind and a μ-Cl.

(22) In the $^1H\{^{31}P\}$ NMR spectra, the signal for H2 appears as a triplet ($^3J_{H-H} = 3.6$ Hz), while that of H1 and H3 appears as a doublet ($^3J_{H-H} = 3.5$ Hz).

The diamagnetism of these d^9 complexes implies a Pd−Pd bond, which is reflected in the relatively short bond distance of ca. 2.60 Å; this is similar to analogous distances of 2.61−2.72 Å found in (μ-allyl)(μ-X)Pd(PPh_3)$_2$ (X = Cl,[23] I,[24] Cp,[25] allyl[26]) and lies within the expected range of 2.53−2.70 Å for Pd^I−Pd^I bond distances found in a large number of compounds.[27] As was alluded to above, H4 and H7 are fairly close to one of the Ph rings of the PPh_3 ligand in **7b**,[28] which helps explain the unusually upfield signals of these protons in the ^{1}NMR spectrum of **7b** (vide supra).

The most notable feature of these complexes is the unusual bonding mode of the indenyl moiety: although there are many precedents for complexes featuring μ-allyl or μ-Cp ligands on a Pd^I−Pd^I framework,[10] the only precedents for the analogous μ,η^3-Ind complexes are the compounds [(μ,η^3-Ind)Pd(CNR)]$_2$ (R = *t*-Bu; 2,6-$(CH_3)_2C_6H_3$; 2,4,6-$(CH_3)_3C_6H_2$; 2,4,6-(*t*-Bu)$_3C_6H_2$)).[8c,d] The μ,η^3-Ind ligands in **7a** and **7b** are symmetrically bonded to the two Pd^I centers and show Pd−C distances identical to those observed in the [(μ,η^3-Ind)Pd(CNR)]$_2$ analogues (Pd1−C1 ≈ Pd2−C3 ≈ 2.1 Å and Pd1−C2 ≈ Pd2−C2 ≈ 2.4 Å). The relatively long Pd1−C7a and Pd2−C3a distances of ca. 2.9 Å are out of the normal bonding range and support the trihapto designation. Indeed, the ΔM−C values observed for **7a** and **7b** (0.83 and 0.87 Å, respectively; Table 4) are in the same range as those found previously in η^3-Ind complexes[29] and much larger than those of the previously described monomeric (η^{3-5}-Ind)Pd^{II} complexes **2**. On the other hand, the hinge and fold angles in **7** are fairly small, representing only small planar distortions for the Ind ligands (**7a**, HA ≈ 6°, FA ≈ 12°; **7b**, HA ≈ 2°, FA ≈ 5°).

Another interesting feature of the crystal structure in complex **7a** is the presence of a cocrystallized half-molecule of *trans*-1,1′-bis(indenylidene) (Figure 6). The two Ind moieties in this molecule are linked by a double bond (C81═C81^{i})[30] involving a trans configuration imposed by the inversion center. The distances and angles are comparable to those obtained for the recently published structure of *trans*-1,1′-bis(indenylidene).[31] As mentioned earlier, we believe that this side product arises from the Pd^0-catalyzed dehydrogenation of Ind−Ind, which is generated in situ during the formation of **7**.

(23) Sieller, J.; Svensson, A.; Lindqvist, O. *J. Organomet. Chem.* **1987**, *320*, 129.
(24) Kobayashi, Y.; Iataka, Y.; Yamazaki, H. *Acta Crystallogr.* **1972**, *B28*, 899.
(25) (a) Werner, H.; Kuhn, A.; Tune, D. J. Kruger, C.; Brauer, D. J.; Sekutowski, J. C.; Tsay, Y.-H. *Chem. Ber.* **1977**, *110*, 1763. (b) Werner, H.; Tune, D.; Parker, G.; Kruger, C.; Brauer, D. J. *Angew. Chem., Int. Ed. Engl.* **1975**, *14*, 185.
(26) Jolly, P. W.; Kruger, C.; Schick, K.-P.; Wilke, G. *Z. Naturforsch.* **1985**, *35b*, 926.
(27) (a) Yamamoto, Y.; Yamakazi, H. *Bull. Chem. Soc. Jpn.* **1985**, *58*, 1843. (b) Yamamoto, Y.; Yamakazi, H. *Inorg. Chem.* **1986**, *25*, 3327. (c) Holloway, R. G.; Penfold, B. R.; Colton, R.; McCormich, M. J. *J. Chem. Soc., Chem. Commun.* **1976**, 485. (d) Kullberg, M. L.; Lemke, F. R.; Powell, D. R.; Kubiak, C. P. *Inorg. Chem.* **1985**, *24*, 3589.
(28) The distance from H4 to the Ph group (C41−C42−C43−C44−C45−C46) is 2.771 Å, and that from H7 to the Ph group (C11−C12−C13−C14−C15−C16) is 3.347 Å. By comparison, the distance from H1 to the Ph group (C21−C22−C23−C24−C25−C26) is 3.511 Å, and that from H3 to the Ph group (C41−C42−C43−C44−C45−C46) is 3.968 Å. Protons H5 and H6 are too far from the closest Ph group (>4 Å).
(29) Examples include (η^5-Ind)(η^3-Ind)W$(CO)_2$ (ΔM−C = 0.07 and 0.72 Å) (Nesmeyanov, A. W.; Ustynyuk, N. A.; Makarova, L. G.; Andrianov, V. G.; Struchkov, Y. T.; Andrae, S.; Ustynyuk, Y. A.; Malyugina, S. G. *J. Organomet. Chem.* **1978**, *159*, 189) and (η^3-Ind)Ir$(PMe_3)_3$ (ΔM−C = 0.79 Å) (ref 19). For detailed discussions of Ind hapticity, see refs 15a,b.
(30) Symmetry code: (i) $-x + 1, -y, -z + 2$.
(31) Caparelli, M. V.; Machado, R.; De Sanctis, Y.; Arce, A. J. *Acta Crystallogr.* **1996**, *C52*, 947.

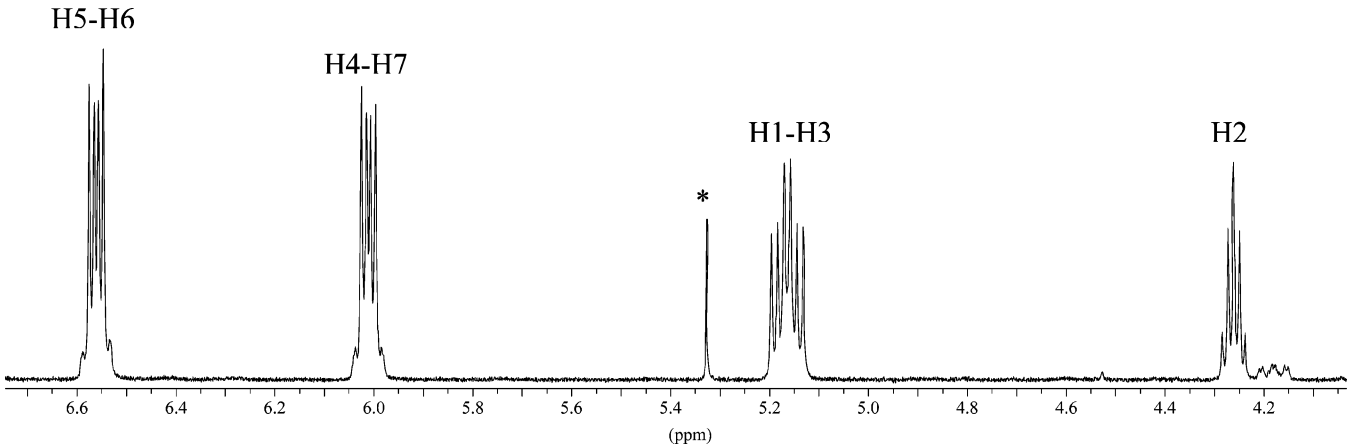

Figure 7. 300 MHz ^{1}H NMR spectrum of complex **7b** in $CDCl_3$ (*, trace CH_2Cl_2).

Table 3. Crystal Data, Data Collection, and Structure Refinement Parameters of **7a**, **7b**, and **8a**

	7a	7b	8a
formula	$C_{54}H_{79}ClP_2Pd_2$	$C_{45}H_{37}ClP_2Pd_2$	$C_{25}H_{42}Cl_2N_1P_1Pd_1$
mol wt	1038.36	887.94	564.87
cryst color, habit	orange, block	red, block	yellow, block
cryst dimens, mm	0.12 × 0.17 × 0.34	0.29 × 0.30 × 0.51	0.20 × 0.30 × 0.42
system	monoclinic	monoclinic	monoclinic
space group	$P2_1/n$	Cc	$P2_1/c$
a, Å	17.481(3)	13.8689(3)	17.0179(2)
b, Å	16.598(3)	14.2117(3)	9.4258(1)
c, Å	17.740(3)	19.1372(6)	18.1497(3)
α, deg	90	90	90
β, deg	109.518(7)	104.345(2)	115.208(1)
γ, deg	90	90	90
volume, Å^3	4851.6(13)	3654.35(16)	2634.09(6)
Z	4	4	4
D(calcd), g cm^{-1}	1.422	1.614	1.424
diffractometer	Bruker AXS, Smart 2K	Bruker AXS, Smart 2K	Bruker AXS, Smart 2K
temp, K	100	220	100
λ, Å	1.54178	1.54178	1.54178
μ, mm^{-1}	7.363	9.684	8.201
scan type	ω scan	ω scan	ω scan
F(000)	2168	1784	1176
θ_{max}, deg	53.43	72.95	72.84
h,k,l range	$-18 \le h \le 18$	$-16 \le h \le 17$	$-20 \le h \le 21$
	$-17 \le k \le 17$	$-17 \le k \le 17$	$-11 \le k \le 11$
	$-18 \le l \le 18$	$-22 \le l \le 19$	$-21 \le l \le 19$
no. of reflns collected/unique	59 157/5653	14 769/5858	21 228/5049
absorption	multiscans	multiscans	multiscans
correction	SADABS	SADABS	SADABS
T (min, max)	0.08, 0.29	0.06, 0.22	0.19, 0.37
R [$F^2 > 2\sigma(F^2)$], $R_w(F^2)$	0.0549, 0.1253	0.0535, 0.1369	0.0308, 0.0798
GOF	0.976	1.041	1.039

Conclusion

The reaction of the dimer [(η^3-Ind)Pd(μ-Cl)]$_2$ (**1**) with a variety of ligands has resulted in the formation of complexes featuring Ind ligands of different hapticities, underlining the influence of the auxiliary ligand(s) on the hapticity of Ind. Thus, reaction with phosphines or NEt_3 gives (η^{3-5}-Ind)Pd(L)Cl (**2** and **3**), whereas ^{t}BuNC, $BnNH_2$, and pyridine give the η^1-Ind complexes [(η^1-Ind)(*t*-BuNC)Pd(μ-Cl)]$_2$ or *trans*-(η^1-Ind)PdL_2-Cl (L = $BnNH_2$ (**4**), py (**5**)). On the other hand, the one-pot reaction of **1** with a mixture of $BnNH_2$ and the phosphine ligands PCy_3 or PPh_3 gave the mixed-ligand amino and phosphine species (η^1-Ind)Pd(PR_3)($BnNH_2$)Cl (**6**), which can also be prepared by addition of $BnNH_2$ to (η-Ind)Pd(PR_3)Cl (**2**). Compounds **6** serve as models for the postulated intermediates in the associative ligand displacement reactions (η-Ind)M(L)-Cl + L′ → (η-Ind)M(L′)Cl + L.

Gradual decomposition of **6** in solution generates the dinuclear Pd^I compounds (μ,η^3-Ind)(μ-Cl)Pd$_2$(PR_3)$_2$ (**7**), displaying a rare mode of Ind hapticity. A brief examination of the reactivities of these new species with $AgBF_4$ or MeMgCl has shown that they give, respectively, the monomeric products [(η-Ind)Pd(PPh_3)$_2$][BF_4] and (η-Ind)Pd(PPh_3)Me plus the (undetected) fragment Pd(PR_3)$_n$. Our preliminary observations suggest that complexes **7** are formed via a comproportionation reaction from Ind−Pd^{II} and Pd^0(PR_3)$_n$ species and undergo spontaneous disproportionation reaction to regenerate these precursors. These results suggest that the possibility of such disproportionation reactions occurring in other Pd^I−Pd^I complexes should be taken into account, especially in view of the recent reports on the catalytic reactivities exhibited by some of these complexes.[32] We continue to probe further this issue, in particular, and the chemistry of these μ,η^3-Ind compounds in general.

Table 4. Selected Bond Distances (Å) and Angles (deg) for **7a** and **7b**

	7a	7b
Pd1−Cl	2.4301(19)	2.411(2)
Pd1−P1	2.293(2)	2.260(2)
Pd1−C1	2.107(7)	2.072(7)
Pd1−C2	2.425(7)	2.405(7)
Pd2−Cl	2.4207(19)	2.432(2)
Pd2−P2	2.280(2)	2.274(2)
Pd2−C2	2.412(7)	2.401(8)
Pd2−C3	2.106(7)	2.122(7)
Pd1−C7a	2.988(7)	2.929(8)
Pd2−C3a	2.974(7)	2.930(7)
Pd1−Pd2	2.5971(8)	2.6031(6)
C1−C2	1.418(10)	1.422(11)
C2−C3	1.415(10)	1.427(11)
C3−C3a	1.496(10)	1.480(12)
C3a−C7a	1.429(11)	1.419(11)
C7a−C1	1.476(10)	1.502(11)
C3a−C4	1.403(10)	1.392(12)
C4−C5	1.379(11)	1.400(15)
C5−C6	1.377(10)	1.391(14)
C6−C7	1.417(10)	1.399(14)
C7−C7a	1.389(10)	1.379(12)
C1−Pd1−P1	103.1(2)	99.9(2)
P1−Pd1−Cl	113.52(7)	115.60(6)
Cl−Pd1−P2	57.45(5)	57.89(5)
Pd2−Pd1−C1	86.0(2)	86.5(2)
C3−Pd2−P2	99.5(2)	101.5(2)
P2−Pd2−Cl	115.42(7)	114.34(7)
Cl−Pd2−Pd1	57.80(5)	57.10(5)
Pd1−Pd2−C3	87.4(2)	87.2(2)
Pd1−Cl−Pd2	64.74(5)	65.01(5)
ΔM−C (Å)[a]	0.87	0.83
HA (deg)	5.61	1.92
FA (deg)	12.49	4.69

[a] ΔM−C = 0.5(Pd1−C7a + Pd2−C3a) − 0.5(Pd1−C1 + Pd2−C3).

Experimental Section

General Comments. All manipulations and experiments were performed under inert atmosphere using standard Schlenk techniques and/or a nitrogen-filled glovebox. Dry, oxygen-free solvents were prepared by distillation from appropriate drying agents and employed throughout. The syntheses of [(η^3-Ind)Pd(μ-Cl)]$_2$ (**1**), (η-Ind)Pd(PR_3)-Cl (**2**), (η-Ind)Pd(PPh_3)Me, and [(η-Ind)Pd(PPh_3)$_2$][BF_4] have been reported previously;[8] all other reagents used in the experiments were obtained from commercial sources and used as received. The elemental analyses were performed by the Laboratoire d'Analyse Elémentaire (Université de Montréal). Bruker AV500, ARX400, AV400, AMX300, and AV300 spectrometers were employed for recording ^{1}H (500, 400, and 300 MHz), ^{13}C{^{1}H} (126, 100, and 75 MHz), and ^{31}P{^{1}H} (202, 161, and 121 MHz) NMR spectra at ambient temperature, unless otherwise specified. The ^{1}H and ^{13}C NMR spectra were referenced to solvent resonances, as follows: 7.26 and 77.16 ppm for C*H*Cl_3 and *C*DCl_3, 7.16 and 128.06 ppm for C_6D_5*H* and *C*$_6D_6$, 5.30 and 53.52 for CD*H*Cl_2 and CD_2Cl_2, 2.11 and 21.10 for C_7D_7*H* and C_7D_8. The ^{31}P NMR spectra were referenced to 85% H_3*P*O_4 (0 ppm).

Crystal Structure Determinations. The crystal data for complexes **3**, **4**, **5**, **6a**, **7a**, **7b**, and **8a** were collected on Bruker AXS Smart 2K and 1K (for **4**) diffractometers using SMART.[33] Graphite-monochromated Cu Kα radiation was used at 100 K for all crystals except those of **7b**, for which the temperature was 220 K, and **4**, for which the radiation used was Mo Kα at 125 K. Cell refinement and data reduction were done using SAINT.[34] All structures were solved by direct methods using SHELXS97[35] and difmap synthesis using SHELXL97;[36] the refinements were done on F^2 by full-matrix least squares. All non-hydrogen atoms were refined anisotropically, while the hydrogens (isotropic) were constrained to the parent atom using a riding model. The crystal data and experimental details are listed in Tables 1 and 3, while selected bond distances and angles are listed in Tables 2 and 4. The Ind moiety and the Cl atom in the crystal structure of **5** were disordered over two positions, with respective occupancy factors of 0.58/0.42 and 0.61/0.39. One of the $BnNH_2$ groups present within the crystal structure of **4** was also disordered over two positions (0.69/0.31). Each of the disorders was refined anisotropically using restraints (SAME/SADI/EADP/DFIX) applied in order to improve the model. The reported structure of **6a** is based on the PLATON/SQUEEZE[37] corrected data (volume of the potential solvent = 168 Å^3; improvement of 4.1% in R1 while correcting for 41 electrons/cell).

Synthesis of (η-Ind)Pd(NEt_3)Cl (3). NEt_3 (441 μL, 3.2 mmol) was added to a stirred C_6H_6 suspension (30 mL) of [(η^3-Ind)Pd(μ-Cl)]$_2$ (**1**; 650 mg, 1.3 mmol) at room temperature. After being stirred for 2 h, the resulting brown solution was concentrated to ca. 5 mL, and 15 mL of hexane was added. A brown powder precipitated and was isolated by filtration and washed with hexane (650 mg, 72%). Recrystallization of a small portion of this solid from a C_6H_6/hexane solution yielded crystals suitable for X-ray diffraction studies and elemental analysis. ^{1}H NMR (C_6D_6, 400 MHz): δ 6.91 (d, $^3J_{H-H}$ = 6.3 Hz, H_7), 6.69 (br, H_5 and H_6), 6.48 (d, $^3J_{H-H}$ = 6.2 Hz, H_4), 6.34 (br, H_2), 5.62 (br, H_1), 4.68 (br, H_3), 2.63−2.49 (m, CH_2), 0.73 (t, $^3J_{H-H}$ = 6.9 Hz, CH_3). ^{1}H NMR (C_7D_8, 500 MHz, 263 K): δ 6.93−6.91 (dd, $^3J_{H7-H6}$ = 7.2 Hz, $^4J_{H7-H1}$ = 0.9 Hz, H_7), 6.69 (quintuplet of doublets, $^3J_{H-H}$ = 7.5 Hz, $^5J_{H-H}$ = 1.2 Hz, H_5 and H_6), 6.45 (dd, $^3J_{H4-H5}$ = 7.3 Hz, $^4J_{H4-H3}$ = 0.9 Hz, H_4), 6.31 (t, $^3J_{H-H}$ = 3.1 Hz, H_2), 5.59 (td, $^3J_{H1-H2}$ = $^4J_{H1-H3}$ = 2.4 Hz, $^4J_{H1-H7}$ = 0.7 Hz, H_1), 4.61 (td, $^3J_{H3-H2}$ = $^4J_{H3-H1}$ = 2.5 Hz, $^4J_{H3-H4}$ = 0.8 Hz, H_3), 2.54 (q, $^3J_{H-H}$ = 6.9 Hz, CH_2), 0.73 (t, $^3J_{H-H}$ = 6.9 Hz, CH_3). ^{13}C{^{1}H} NMR ($CDCl_3$, 75 MHz): δ 139.86 (s, C_{3a} or C_{7a}), 128.50 (s, C_5), 126.62 (s, C_6), 119.33 (s, C_7), 115.97 (s, C_4), 111.22 (s, C_2), 81.56 (s, C_3), 72.72 (s, C_1), 50.02 (s, *C*H$_2$), 10.64 (s, *C*H$_3$). The missing resonance for C3a or C7a is probably obscured under the residual solvent resonances at ca. 129 ppm. Anal. Calcd for $C_{15}H_{22}N_1Cl_1Pd_1$: C, 50.29; H, 6.19; N, 3.91. Found: C, 50.15; H, 6.27; N, 3.76.

Synthesis of (η^1-Ind)Pd($BnNH_2$)$_2$Cl (4). Method A. Benzylamine (127 μL, 1.2 mmol) was added to a stirred C_6H_6 suspension (15 mL) of [(η^3-Ind)Pd(μ-Cl)]$_2$ (**1**; 150 mg, 0.29 mmol) at room temperature. The yellow-green mixture was stirred approximately 2 h, filtered, and evaporated to dryness to give a yellow solid which was washed with hexane (200 mg, 73%). Recrystallization of a small portion of this solid from a C_6H_6/hexane solution yielded crystals suitable for X-ray diffraction studies.

Method B. Benzylamine (61 μL, 0.56 mmol) was added to a stirred C_6H_6 solution (15 mL) of (Ind)Pd(NEt_3)Cl (**3**; 100 mg, 0.28 mmol) at room temperature. After being stirred for 2 h, the resulting brown-green mixture was concentrated to ca. 5 mL. A yellow powder precipitated and was isolated by filtration and washed with hexane (110 mg, 84%). ^{1}H NMR ($CDCl_3$, 400 MHz): δ 7.64 (d, $^3J_{H-H}$ = 7.3 Hz, H_4 or H_7), 7.45 (d, $^3J_{H-H}$ = 7.3 Hz, H_7 or H_4), 7.36−7.28 (m, Ph), 7.23 (t, $^3J_{H-H}$ = 7.4 Hz, H_6 or H_5), 7.17 (t, $^3J_{H-H}$ = 7.4 Hz, H_5 or H_6), 7.11−7.08 (m, Ph), 6.82 (d, $^3J_{H-H}$ = 5.0 Hz, H_3), 6.62 (dd, $^3J_{H-H}$ = 5.0 Hz and $^3J_{H-H}$ = 1.9 Hz, H_2), 4.72 (d, $^3J_{H-H}$ = 1.8 Hz, H_1), 3.84, 3.34 (td, $^3J_{H-H}$ = 12.4 Hz and $^2J_{H-H}$ = 3.9 Hz, CH_2), 2.37, 1.61 (brt,

(32) (a) Stambouli, J. P.; Kuwano, R.; Hartwig J. F. *Angew. Chem., Int. Ed.* **2002**, *41*, 4746. (b) Prashad, M.; Mak, X. Y.; Liu, Y.; Repic, O. *J. Org. Chem.* **2003**, *68*, 1163. (c) Christmann, U.; Vilar, R.; White, A. J. P.; Williams, D. J. *Chem. Commun.* **2004**, 1294.
(33) *SMART*, Release 5.059; Bruker Molecular Analysis Research Tool, Bruker AXS Inc.: Madison, WI, 1999.
(34) *SAINT*, Release 6.06; Integration Software for Single-Crystal Data, Bruker AXS Inc.: Madison, WI, 1999.
(35) Sheldrick, G. M. *SHELXS*, Program for the solution of Crystal Structures; University of Goettingen: Goettingen, Germany, 1997.
(36) Sheldrick, G. M. *SHELXL*, Program for the Refinement of Crystal Structures; University of Goettingen: Goettingen, Germany, 1997.
(37) Spek, A. L. *PLATON*; University of Utrecht: Utrecht, The Netherlands, 2002.

$^3J_{H-H}$ = 11.1 Hz, NH_2). ^{1}H NMR (C_6D_6, 400 MHz): δ 7.70 (d, $^3J_{H-H}$ = 7.3 Hz, H_4 or H_7), 7.40 (d, $^3J_{H-H}$ = 7.3 Hz, H_7 or H_4), 7.19−7.16, 7.04−6.90 (m, Ph, H_5 and H_6), 6.67 (d, $^3J_{H-H}$ = 5.0 Hz, H_3), 6.60 (dd, $^3J_{H-H}$ = 4.9 and 2.1 Hz, H_2), 4.52 (br, H_1) 3.68, 3.13 (td, $^3J_{H-H}$ = 11.8 and $^2J_{H-H}$ = 3.7 Hz, CH_2), 2.13, 1.33 (brt, $^3J_{H-H}$ = 10.0 Hz NH_2). ^{13}C{^{1}H} NMR ($CDCl_3$, 100 MHz): δ 149.62 (s, C_{7a} or C_{3a}), 141.72 (s, C_{3a} or C_{7a}), 138.94 (s, C_{ipso}), 138.76 (s, C_2), 128.97 (s, C_{ortho}), 128.66 (s, C_6 or C_5) 128.22 (s, C_{meta} and C_{para}), 124.44 (s, C_5 or C_6), 123.76 (s, C_4 or C_7), 121.25 (s, C_7 or C_4), 120.75 (s, C_3), 49.44 (s, CH_2), 40.08 (s, C_1). Anal. Calcd for $C_{23}H_{25}Cl_1N_2Pd_1$: C, 58.61; H, 5.35; N, 5.94. Found: C, 59.04; H, 5.28; N, 5.37.

Synthesis of (η^1-Ind)Pd(Py)$_2$Cl (5). Method A. Pyridine (82 μL, 1.0 mmol) was added to a stirred C_6H_6 suspension (25 mL) of [(η^3-Ind)Pd(μ-Cl)]$_2$ (**1**; 130 mg, 0.25 mmol) at room temperature. The yellow-brown mixture was stirred for approximately 2 h, filtered, and evaporated to dryness to give a yellow solid (160 mg, 76%).

Method B. Pyridine (207 μL, 2.6 mmol) was added to a stirred C_6H_6 solution (20 mL) of (Ind)Pd(NEt_3)Cl (**3**; 460 mg, 1.3 mmol) at room temperature. After being stirred for 3 h, the resulting brown-green mixture was concentrated to ca. 10 mL. A yellow powder precipitated and was isolated by filtration and washed with hexane (450 mg, 84%). Recrystallization of a small portion of this solid from a C_6H_6/hexane solution yielded crystals suitable for X-ray diffraction studies.

^{1}H NMR ($CDCl_3$, 400 MHz): δ 8.38 (d, $^3J_{H-H}$ = 6.9 Hz, H_{ortho}), 7.45 (t, $^3J_{H-H}$ = 7.6 Hz, H_{para}), 7.01 (t, $^3J_{H-H}$ = 6.9 Hz, H_{meta}), 6.93−6.72 (m, H_{4-7}), 6.68 (dd, $^3J_{H-H}$ = 4.1 and 1.6 Hz, H_2), 6.45 (d, $^3J_{H-H}$ = 5.1 Hz, H_3), 4.77 (br, H_1). ^{13}C{^{1}H} NMR ($CDCl_3$, 100 MHz): δ 151.72 (s, C_{ortho}), 150.58 (s, C_{7a} or C_{3a}), 142.54 (s, C_{3a} or C_{7a}), 137.28 (s, C_2), 136.94 (s, C_{para}), 124.33 (s, C_{meta}), 123.55 (s, C_3), 127.24, 124.93, 122.84, 120.50 (s, C_{4-7}), 42.54 (s, C_1). Anal. Calcd for $C_{19}H_{17}Cl_1N_2Pd_1 \cdot H_2O$: C, 52.67; H, 4.42; N, 6.47. Found: C, 52.69; H, 3.89; N, 5.97.

Synthesis of (η^1-Ind)Pd(PCy$_3$)(BnNH$_2$)Cl (6a). Method A. Benzylamine (170 μL, 1.56 mmol) was added to a solution of [(η^3-Ind)Pd(μ-Cl)]$_2$ (**1**; 400 mg, 0.78 mmol) in CH_2Cl_2 (30 mL) at room temperature. The brown mixture was stirred for 30 min, and PCy_3 (436 mg, 1.56 mmol) was added. The orange-brown mixture was stirred for approximately 1 h, filtered, and evaporated to dryness to give an orange solid (850 mg, 85%).

Method B. $BnNH_2$ (76 μL, 0.7 mmol) was added to a stirred C_6H_6 solution (20 mL) of (Ind)Pd(PCy_3)Cl (**2a**; 375 mg, 0.7 mmol) at room temperature. After being stirred for 2 h, the resulting orange solution was evaporated to dryness, and 10 mL of hexane was added. An orange powder precipitated and was isolated by filtration (350 mg, 78%). Recrystallization of this solid from a cold hexane solution yielded crystals of (η^1-Ind)Pd(PCy_3)(BnNH$_2$)Cl (**6a**), (μ,η^3-Ind)(μ-Cl)Pd$_2$(PCy_3)$_2$ (**7a**), and (BnNH$_2$)(PCy_3)PdCl$_2$ (**8a**) suitable for X-ray diffraction studies and elemental analysis.

6a. ^{1}H NMR (C_6D_6, 300 MHz): δ 7.95, 7.41, 6.98, 6.82, 6.66 (br, H_{2-7}), 5.03 (br, H_1), 3.85 (br, CH_2), 2.44−1.20 (m, NH_2 and PCy_3). ^{31}P{^{1}H} NMR (C_6D_6, 121 MHz): δ 41.5 (s). ^{1}H NMR (C_7D_8, 500 MHz, 263 K): δ 7.96−7.94, 7.50−7.48, 7.23−6.95 (m, Ph and H_{4-7}), 6.83 (d, $^3J_{H-H}$ = 5.0 Hz, H_2), 6.80−6.78 (m, H_{4-7}), 6.68 (d, $^3J_{H-H}$ = 4.9 Hz, H_3), 4.94 (d, $^3J_{H-P}$ = 5.4 Hz, H_1), 3.82 (t, $^3J_{H-H}$ = 12.9 Hz, CH_2), 3.53 (s, CH_2), 2.44−1.24 (m, NH_2 and PCy_3). ^{13}C{^{1}H} NMR (C_7D_8, 126 MHz, 263 K): δ 151.76 (s, C_{7a}), 144.68 (s, C_{3a}), 138.94 (s, C_{ipso}), 129.53, 129.02, 128.83, 128.69, 128.60, 128.49, 127.82, 127.65, 127.06, 125.77, 124.84, 124.62, 123.94, 121.74, 121.69 (s, Ph and C_{2-7}), 48.77, 47.26 (s, CH_2), 38.85 (s, C_1), 34.61 (d, $^1J_{C-P}$ = 22.6 Hz, C_{ipso}), 31.09 (d, $^2J_{C-P}$ = 9.4 Hz, C_{ortho}), 28.41 (t, $^3J_{C-P}$ = 9.4 Hz, C_{meta}), 27.48 (s, C_{para}). ^{31}P{^{1}H} NMR (C_7D_8, 202 MHz, 263 K): δ 40.5 (s). Anal. Calcd for $C_{34}H_{49}Cl_1N_1Pd_1$: C, 63.35; H, 7.66; N, 2.17. Found: C, 63.48; H, 7.88; N, 2.05.

Synthesis of (μ,η^3-Ind)(μ-Cl)Pd$_2$(PCy$_3$)$_2$ (7a). After several hours in solution, the complex (BnNH$_2$)(PCy_3)PdCl(η^1-Ind) (**6a**) gave (μ,η^3-Ind)(μ-Cl)Pd(PCy_3)$_2$ (**7a**) as an orange solid. Recrystallization of this solid from a cold hexane solution yielded crystals suitable for X-ray diffraction studies and elemental analysis. ^{1}H NMR (C_6D_6, 400 MHz): δ 7.35 (dd, $^3J_{H-H}$ = 5.6 Hz and $^4J_{H-H}$ = 3.1 Hz, H_5 and H_6), 7.04 (dd, $^3J_{H-H}$ = 5.6 Hz and $^4J_{H-H}$ = 3.1 Hz, H_4 and H_7), 5.81 (td, $^3J_{H-P}$ = 7.3 Hz and $^3J_{H-H}$ = 3.8 Hz, H_1 and H_3), 4.22 (quintuplet, $^3J_{H-H}$ = $^3J_{H-P}$ = 3.6 Hz, H_2), 2.04−1.05 (m, PCy_3). ^{31}P{^{1}H} NMR (C_6D_6, 161.92 MHz): δ 38.5 (s). ^{1}H NMR (CD_2Cl_2, 500 MHz, 263 K): δ 6.97 (dd, $^4J_{H-H}$ = 3.0 Hz and $^3J_{H-H}$ = 5.5 Hz, H_5 and H_6), 6.72 (dd, $^3J_{H-H}$ = 5.4 Hz and $^4J_{H-H}$ = 3.1 Hz, H_4 and H_7), 5.44 (td, $^3J_{H-P}$ = 7.2 Hz and $^3J_{H-H}$ = 3.9 Hz, H_1 and H_3), 3.75 (quintuplet, $^3J_{H-H}$ = $^3J_{H-P}$ = 3.5 Hz, H_2), 2.01−0.83 (m, PCy_3). ^{13}C{^{1}H} NMR (CD_2Cl_2, 126 MHz, 263 K): δ 145.68 (s, C_{7a} and C_{3a}), 122.84 (s, C_4 and C_7), 121.82 (s, C_5 and C_6), 71.19 (s, C_2), 48.99 (s, C_1 and C_3), 34.64 (t, $^1J_{C-P}$ = 7.6 Hz, C_{ipso}), 30.11 (s, C_{ortho}), 27.35 (s, C_{meta}), 26.15 (s, C_{para}). ^{31}P{^{1}H} NMR (CD_2Cl_2, 202 MHz, 263 K): δ 37.7 (s). Anal. Calcd for $C_{45}H_{73}Cl_1P_2Pd_2 \cdot 0.5C_{18}H_{12}$: C, 62.46; H, 7.67. Found: C, 62.39; H, 7.93.

Synthesis of (BnNH$_2$)(PCy$_3$)PdCl$_2$ (8a). Recrystallization of (η^1-Ind)Pd(PCy_3)(BnNH$_2$)Cl (**6a**) in hexane gave yellow crystals, which were identified as the complex (BnNH$_2$)(PCy_3)PdCl$_2$ (**8a**) on the basis of the NMR spectra and X-ray analysis. ^{1}H NMR (C_6D_6, 300 MHz): δ 7.40, 6.98, 6.87 (br, C_6H_5), 3.83 (br, CH_2), 2.54−1.22 (m, NH_2 and PCy_3). ^{31}P{^{1}H} NMR (C_6D_6, 121 MHz): δ 44.11 (s).

(η^1-Ind)Pd(BnNH$_2$)(PPh$_3$)Cl (6b), (μ,η^3-Ind)(μ-Cl)Pd$_2$(PPh$_3$)$_2$ (7b), and (BnNH$_2$)(PPh$_3$)PdCl$_2$ (8b). NMR-scale preparation of **6b** (C_6D_6), either by the reaction of **1** (10 mg, 0.0019 mmol) with a mixture of $BnNH_2$ (4 μL, 0.0039 mmol) and PPh_3 (10 mg, 0.0039 mmol) or by the reaction of **2b** (30 mg, 0.058 mmol) with $BnNH_2$ (8 μL, 0.058 mmol), showed formation of **6b**. Monitoring these samples indicated that the initially formed **6b** is gradually converted to **7b** and **8b** after a few hours. All attempts at purifying the mixtures obtained from large-scale reactions led to the isolation of pure samples of **7b** only. Therefore, **7b** has been characterized fully (vide infra), whereas **6b** and **8b** were characterized by NMR spectra only, as described below.

6b. ^{1}H NMR (C_6D_6, 300 MHz): δ 8.01−7.97 (m, PPh_3), 7.48, 7.31 (d, $^3J_{H-H}$ = 7.0 Hz, H_4 and H_7), 7.1−6.8 (m, PPh_3, H_5 and H_6), 6.55 (d, $^3J_{H-H}$ = 5.1 Hz, H_3), 6.44 (d, $^3J_{H-H}$ = 6.1 Hz, H_2), 4.55 (d, $^3J_{H-P}$ = 6.0 Hz, H_1), 3.86, 3.38 (br, NH_2), 2.53, 2.13 (br, CH_2). ^{1}H NMR (C_7D_8, 126 MHz, 263 K): δ 8.00−7.96 (m, PPh_3), 7.46 (d, $^3J_{H-H}$ = 6.7 Hz, H_4 or H_7), 7.38 (d, $^3J_{H-H}$ = 7.2 Hz, H_7 or H_4), 7.2−6.9 (m, PPh_3 and H_{5-6}), 6.80 (d, $^3J_{H-H}$ = 4.6 Hz, Ph and H_{5-6}), 6.56 (d, $^3J_{H-H}$ = 4.6 Hz, H_3), 6.42 (d, $^3J_{H-H}$ = 3.7 Hz, H_2), 4.47 (d, $^3J_{H-P}$ = 7.6 Hz, H_1), 3.92, 3.54, 2.28 (br, CH_2), 3.28, 0.74, 0.25 (br, NH_2). ^{13}C{^{1}H} NMR (C_7D_8, 126 MHz, 263 K): δ 150.8 (s, C_{7a}), 143.00 (s, C_{3a}), 141.19 (s, C_{ipso} $BnNH_2$), 139.78 (s, C_2), 135.71 (d, $^2J_{C-P}$ = 11.3 Hz, C_{ortho} PPh_3), 132.33 (d, $^1J_{C-P}$ = 49.0 Hz, C_{ipso} PPh_3), 131.27 (s, C_{para} PPh_3), 129.34 (s, C_{ortho} $BnNH_2$), 129.16 (d, $^3J_{C-P}$ = 10.4 Hz, C_{meta} PPh_3), 129.00 (s, C_{meta} $BnNH_2$), 127.93 (s, C_{para} $BnNH_2$), 124.93, 124.78, 124.30, 122.00, 121.85 (s, C_{3-7}), 48.99 (s, CH_2), 46.60 (s, C_1). ^{1}P{^{1}H} NMR (C_6D_6, 161 MHz): δ 37.1 (s). ^{31}P{^{1}H} NMR (C_7D_8, 202 MHz, 263 K): δ 37.0 (s).

Isolation of 7b. Method A. Benzylamine (127 μL, 1.16 mmol) was added to a solution of [(η^3-Ind)Pd(μ-Cl)]$_2$ (**1**; 300 mg, 0.58 mmol) in CH_2Cl_2 (25 mL) at room temperature. The brown mixture was stirred for 10 min, and PPh_3 (303 mg, 1.16 mmol) was added. The resulting brown-red mixture was stirred for approximately 1 h, filtered, and evaporated to dryness. The orange residue was dissolved in CH_2Cl_2 (15 mL) and layered with hexane (10 mL) to give an orange precipitate, which was isolated as a fine powder by filtration (250 mg, 48%). Recrystallization of a small portion of this powder from a $CHCl_3$/hexane solution yielded crystals suitable for X-ray diffraction studies and elemental analysis.

Method B. $BnNH_2$ (31 μL, 0.29 mmol) was added to a stirred C_6H_6 solution (15 mL) of (Ind)Pd(PPh_3)Cl (**2b**; 150 mg, 0.29 mmol) at room temperature. After being stirred for 2 h, the resulting orange solution was evaporated to dryness, and 10 mL of hexane was added. An orange powder precipitated and was isolated by filtration (70 mg, 55%). ^{1}H

NMR ($CDCl_3$, 400 MHz): δ 7.69−7.64 (m, PPh_3), 7.48−7.38 (m, PPh_3), 6.52 (dd, $^3J_{H-H} = 5.4$ Hz and $^4J_{H-H} = 3.1$ Hz, H_5 and H_6), 5.98 (dd, $^3J_{H-H} = 5.4$ Hz and $^4J_{H-H} = 3.1$ Hz, H_4 and H_7), 5.12 (td, $^3J_{H-P} = 7.7$ Hz and $^3J_{H-H} = 3.7$ Hz, H_1 and H_3), 4.22 (quintuplet, $^3J_{H-H} = 3.4$ Hz, H_2). $^{13}C\{^1H\}$ NMR ($CDCl_3$, 100 MHz): δ 143.68 (s, C_{7a} and C_{3a}), 134.69 (t, $^2J_{C-P} = 7.4$ Hz, C_{ortho}), 134.62 (d, $^1J_{C-P} = 43.1$ Hz, C_{ipso}), 130.29 (s, C_{para}), 129.00 (t, $^3J_{C-P} = 4.9$ Hz, C_{meta}), 124.09 (s, C_5 and C_6), 121.62 (s, C_4 and C_7), 78.36 (s, C_2), 57.75 (s, C_1 and C_3). $^{31}P\{^1H\}$ NMR ($CDCl_3$, 121 MHz): δ 25.7 (s). Anal. Calcd for $C_{45}H_{37}Cl_1P_2Pd_2$: C, 60.86; H, 4.20. Found: C, 60.32; H, 4.13.

8b. ^1H NMR (C_6D_6, 300 MHz): δ 7.73−7.27 (m, C_6H_5), 4.13 (br, CH_2), 3.02 (br, NH_2). $^{31}P\{^1H\}$ NMR (C_6D_6, 121 MHz): δ 28.59 (s).

Reaction of Complex 7b with $AgBF_4$. A mixture of (μ,η^3-Ind)(μ-Cl)$Pd_2(PPh_3)_2$ (**7b**; 140 mg, 0.16 mmol) and $AgBF_4$ (31 mg, 0.16 mmol) was stirred in CH_2Cl_2 (20 mL) for 2 h at room temperature and filtered to remove AgCl. Concentration of the filtrate to ca. 5 mL, followed by addition of ca. 15 mL of Et_2O, gave [(η-Ind)$Pd(PPh_3)_2$]BF_4 as an orange precipitate, which was isolated by filtration (60 mg, 46%).

Reaction of Complex 7b with MeMgCl. This reaction was monitored by spectroscopy, without isolating the resulting products. A solution of MeMgCl (4 μL of a 3 M solution in THF) was added at room temperature to a 1 mL C_6D_6 solution of (μ,η^3-Ind)(μ-Cl)$Pd_2(PPh_3)_2$ (**7b**; 10 mg, 0.011 mmol) in an NMR tube. The NMR spectra of this sample showed the complete conversion of **7b** to (η-Ind)$Pd(PPh_3)$Me.

Acknowledgment. This work was made possible by financial support provided by the Natural Sciences and Engineering Research Council of Canada (operating grants to D.Z.) and Université de Montréal (scholarships to C.S.-S.). We are also indebted to Johnson Matthey for the generous loan of $PdCl_2$, and to Dr. M. Simard and F. Bélanger-Gariépy for their assistance with the X-ray analyses.

Supporting Information Available: X-ray crystallographic data, in CIF format, for **3**, **4**, **5**, **6a**, **7a**, **7b**, and **8a**. This material is available free of charge via the Internet at http://pubs.acs.org. Complete details of the X-ray analysis of these compounds, including tables of crystal data, collection and refinement parameters, bond distances and angles, anisotropic thermal parameters, and hydrogen atoms coordinates, have been deposited at the Cambridge Crystallographic Data Centre (CCDC 296295−296301). These data can be obtained free of charge via www.ccdc.cam.ac.uk/data_request/cif, by emailing data_request@ccdc.cam.ac.uk, or by contacting the Cambridge Crystallographic Data Centre, 12, Union Rd., Cambridge CB2 1EZ, UK; fax +44 1223 336033.

JA060747A